SAND 2000-1578C

Nested Acceleration Algorithm for Self-Adjoint Angular Flux Boltzmann-CSD Equation

J. Liscum-Powell (Sandia*, University of New Mexico), A. K. Prinja (University of New Mexico), J. E. Morel (LANL) and L. J. Lorence, Jr.(Sandia*)

The second-order, self-adjoint angular flux (SAAF) equation,[1] modified to include continuous slowing down (CSD), was recently used for coupled electron-photon transport.[2] Results using the standard discrete ordinates approach with linear continuous (LC) spatial finite elements, diamond difference (DD) in energy and DSA source iteration acceleration, generally compared very favorably against the first-order form of the transport equation.[2] However, DD in energy discretization of the CSD operator did not always yield stable, positive solutions for energy spectra and charge deposition, particularly for monoenergetic incident electrons. Here we investigate the numerical solution of the SAAF equation using a higher order, linear discontinuous (LD) discretization in energy with particular emphasis on jointly accelerating the source iteration and within group upscatter introduced by the LD discretization. The angular flux in energy group g is expressed as $\Psi_n(x,E) = \Psi^A_{n,g}(x) + \frac{2}{\Delta E_g}(E-E_g)\Psi^E_{n,g}(x)$, where $\Psi^A_{n,g}(x)$ is the average and $\Psi^E_{n,g}(x)$ the slope angular flux. Applying the Galerkin procedure in energy, the SAAF equation reduces to the following coupled equations

$$\begin{aligned} -\mu_n^2\frac{\partial}{\partial x}\left(\frac{1}{\sigma^A_{R,g}}\frac{\partial\Psi^A_{n,g}}{\partial x}\right) + \sigma^A_{R,g}\Psi^A_{n,g} &= Q^S_{n,g} - \mu_n\frac{\partial}{\partial x}\left(\frac{1}{\sigma^A_{R,g}}Q^S_{n,g}\right) + q_{n,g} - \mu_n\frac{\partial}{\partial x}\left(\frac{1}{\sigma^A_{R,g}}q_{n,g}\right) \\ +\frac{S_{g-1}}{\Delta E_g}\left[\Psi^A_{n,g-1} - \Psi^E_{n,g-1}\right] &- \mu_n\frac{\partial}{\partial x}\left(\frac{1}{\sigma^A_{R,g}}\frac{S_{g-1}}{\Delta E_g}\left[\Psi^A_{n,g-1} - \Psi^E_{n,g-1}\right]\right) \\ +\frac{S_g}{\Delta E_g}\Psi^E_{n,g} &- \mu_n\frac{\partial}{\partial x}\left(\frac{1}{\sigma^A_{R,g}}\frac{S_g}{\Delta E_g}\Psi^E_{n,g}\right) \end{aligned} \quad (1)$$

$$\begin{aligned} -\mu_n^2\frac{\partial}{\partial x}\left(\frac{1}{\sigma^E_{R,g}}\frac{\partial\Psi^E_{n,g}}{\partial x}\right) + \sigma^E_{R,g}\Psi^E_{n,g} &= 3\frac{S_{g-1}}{\Delta E_g}\left[\Psi^A_{n,g-1} - \Psi^E_{n,g-1}\right] \\ &- \mu_n\frac{\partial}{\partial x}\left(\frac{1}{\sigma^E_{R,g}}3\frac{S_{g-1}}{\Delta E_g}\left[\Psi^A_{n,g-1} - \Psi^E_{n,g-1}\right]\right) \\ &- 3\frac{S_g}{\Delta E_g}\Psi^A_{n,g} + \mu_n\frac{\partial}{\partial x}\left(\frac{1}{\sigma^E_{R,g}}3\frac{S_g}{\Delta E_g}\Psi^A_{n,g}\right) \end{aligned} \quad (2)$$

where $Q^S_{n,g}$ is the scattering source and S_g is the group stopping power. The coupling is akin to within group upscatter and introduces an additional level of iteration. For a pure CSD problem, spatially analytic Fourier analysis shows the spectral radius of this iteration to be unity with the offending error mode at zero

DISCLAIMER

DISCLAIMER

wavenumber, consistent with earlier observations based on the first order form of the transport equation.[3] An acceleration scheme which effectively damps out the flat mode is obtained by neglecting all spatial derivatives in the slope flux error. Thus, with the average and slope flux errors defined by $f_{n,g}^{A,E(j+1/2)} = \Psi_{n,g}^{A,E} - \Psi_{n,g}^{A,E(j+1/2)}$, where j is the upscatter iteration index, the lower order error correction equations read

$$\begin{aligned} -\mu_n^2 \frac{d}{dx}\left(\frac{1}{\sigma_{R,g}^A}\frac{df_{n,g}^{A(j+1/2)}}{dx}\right) &- \mu_n \frac{d}{dx}\left(3\frac{\mathcal{S}_g^2}{\sigma_{R,g}^A \sigma_{R,g}^E} f_{n,g}^{A(j+1/2)}\right) \\ +\left(\sigma_{R,g}^A + 3\frac{\mathcal{S}_g^2}{\sigma_{R,g}^E}\right) f_{n,g}^{A(j+1/2)} &= \mathcal{S}_g \left[\Psi_{n,g}^{E(j+1/2)} - \Psi_{n,g}^{E(j)}\right] \\ &- \mu_n \frac{d}{dx}\left(\frac{\mathcal{S}_g}{\sigma_{R,g}^A}\left[\Psi_{n,g}^{E(j+1/2)} - \Psi_{n,g}^{E(j)}\right]\right) \end{aligned} \tag{3}$$

$$f_{n,g}^{E(j+1/2)} = -3\frac{\mathcal{S}_g}{\sigma_{R,g}^E} f_{n,g}^{A(j+1/2)} \tag{4}$$

where $\mathcal{S}_g = \frac{S_g}{\Delta E_g}$. The updated fluxes are then given by $\Psi_{n,g}^{A,E(j+1)} = \Psi_{n,g}^{A,E(j+1/2)} + f_{n,g}^{A,E(j+1/2)}$. This error correction is equivalent to a DD approximation of the CSD term, and the accelerated system has a theoretical spectral radius of 0.20.

A multigroup 1-D S_n code, DOET$_{1D}$, has been developed with LC in space and LD in energy finite element discretization in conjunction with DSA and within group upscatter acceleration. The LC spatial representation yields a coupled set of symmetric, positive-definite algebraic systems for the cell-edge unknown average and slope fluxes, which are solved for each group and along each direction. The nested acceleration algorithm consists of two acceleration schemes which were initially tested individually and the spectral radii numerically estimated, with representative results obtained for 1.0 MeV electrons incident on an Al slab with P_0 and S_8 quadrature. The top graph in Figure 1 shows the estimated DSA spectral radius as a function of iteration number, incorporating DSA and *unaccelerated* upscatter iteration for several energy groups. Each iteration in this plot consists of as many source iterations as necessary to converge on $Q_{n,g}^S$ for a given $\Psi_{n,g}^E$ followed by one upscatter iteration. DSA clearly remains effective in the presence of the outer or upscatter iterations, with spectral radius values considerably less than the theoretical value 0.225. Likewise, the bottom graph in Figure 1 depicts the accelerated upscatter iteration spectral radius with *unaccelerated* source iteration where the iteration on the x-axis consists of as many upscatter iterations as necessary to reach convergence on $\Psi^E_{n,g}$ for a given $Q^S_{n,g}$. The upscatter iterations are effectively accelerated and the spectral radius is bounded from above by the theoretical value of 0.2.

With nested acceleration active, extensive numerical testing shows that the computationally most efficient algorithm is achieved by performing at most two iterations at each level. That is, it is less efficient to fully converge the inner source iterations for each outer upscatter iteration. For the specific example above, the latter approach takes 14.5 seconds on a 550 MHz PC compared to 5.7 seconds for the optimum case. Finally, Figure 2 presents the charge deposition for 100 keV photons on a Gold\Silicon Slab with P_7 scattering and S_8 quadrature. The profile depicted in Figure 2 indicates excellent agreement with ONEBFP and validates our approach.

References

[1] J. E. Morel and J. M. McGhee. A Self-Adjoint Angular Flux Equation. *NSE*, 132:312–325, 1999.

[2] J. L. Liscum-Powell, A. K. Prinja, J. E. Morel, and L. J. Lorence, Jr. Self-Adjoint Angular Flux Equation for Coupled Electron-Photon Transport. *Transactions of the American Nuclear Society*, 81:129–130, 1999.

[3] M. S. Lazo and J. E. Morel. A Linear Discontinuous Galerkin Approximation for the Continuous Slowing Down Operator. *NSE*, 92:98–109, 1986.

*Sandia is a multiprogram laboratory operated by Sandia Corporation, a Lockheed Martin Company, for the United States Department of Energy under Contract DE-AC04-94AL85000.

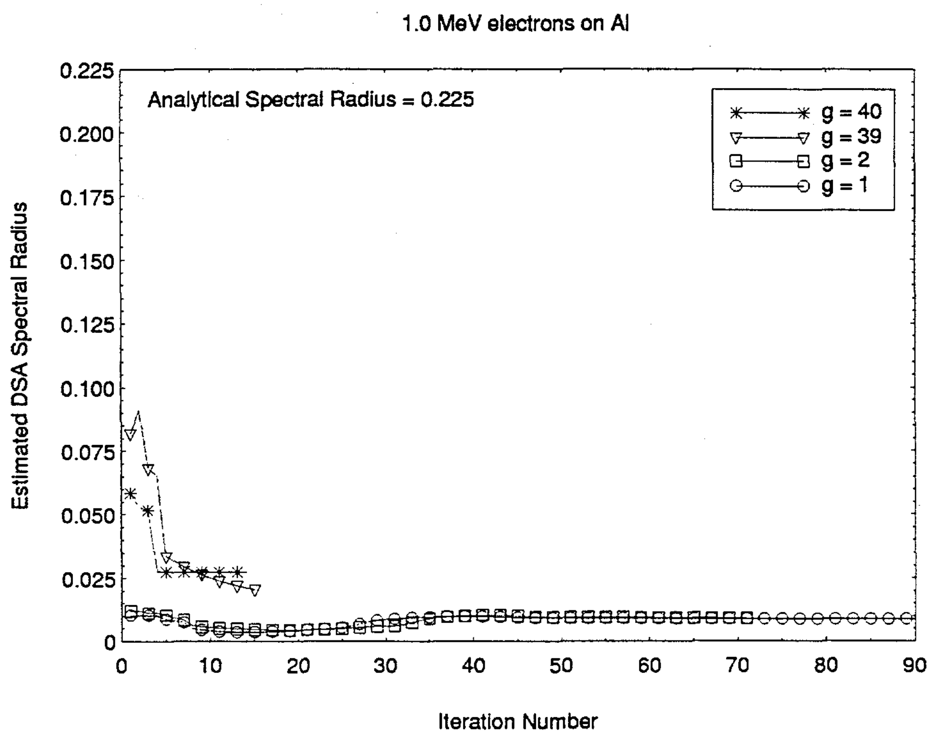

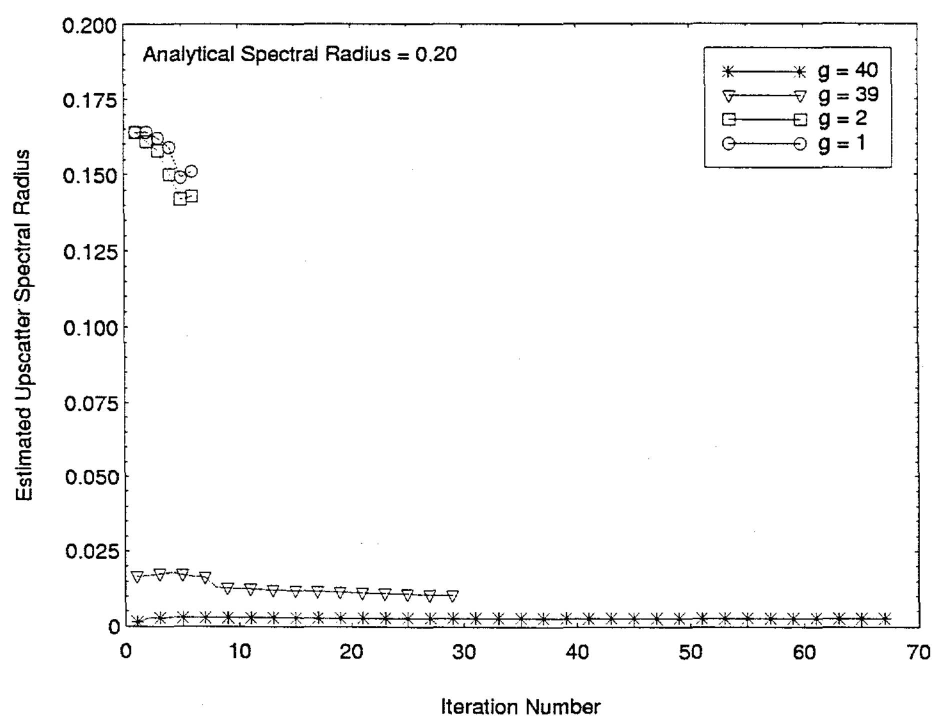

Figure 1: Estimated DSA and Upscatter Spectral Radius

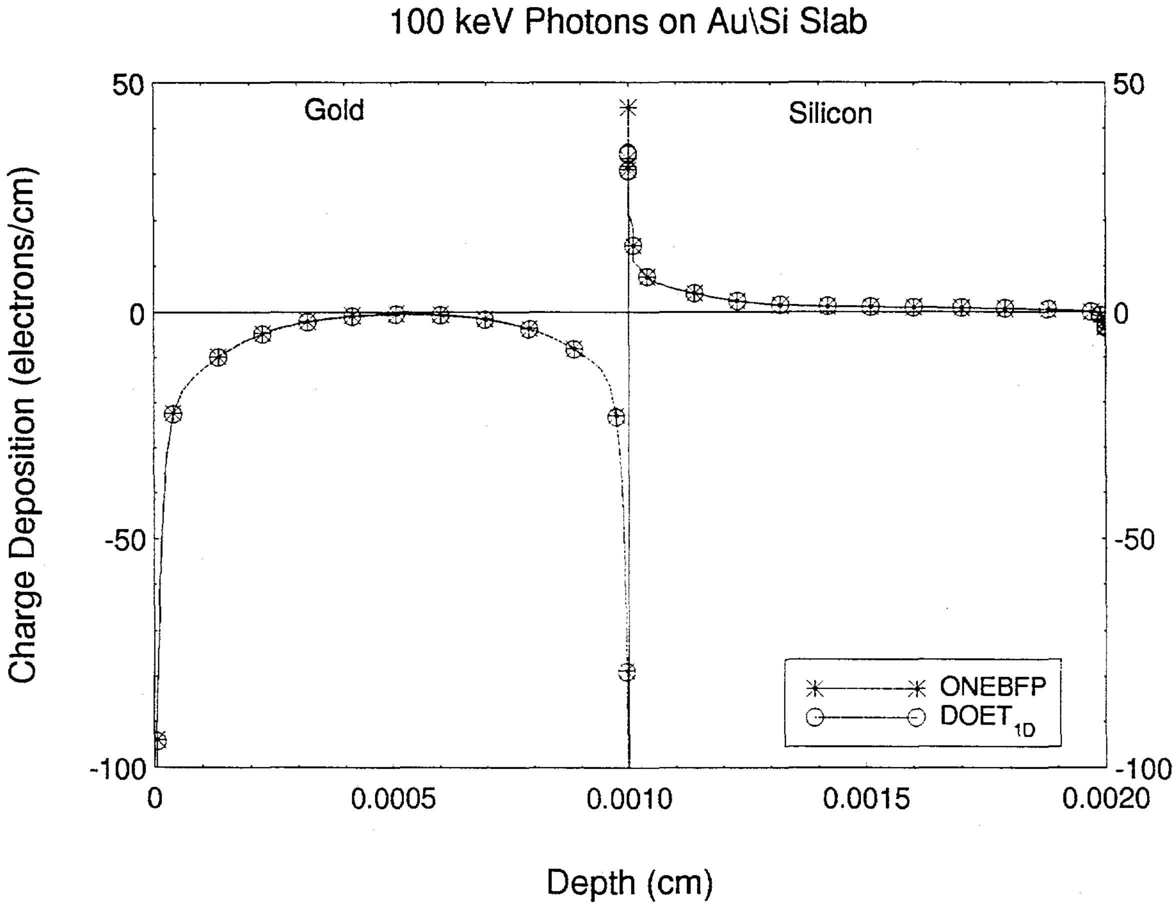

Figure 2: Charge Deposition Profile for 100 keV Photons on Au\Si